Resolving Deep-Water Stratigraphic Traps: Forward Seismic Modeling of a Turbidite Onlap; Montagne de Chalufy, Grès d'Annot Formation, Southeast France

Stanbrook, David A.
Maersk Olie og Gas A/S
Esplanaden 50
1098 København K
Denmark
e-mail: dast@maerskoil.com

Pringle, Jamie K.
School of Physical Sciences & Geography
Keele University
Keele, Staffs. ST5 5BG, UK

Elliott, Trevor
Department of Earth and Ocean Sciences
University of Liverpool
4 Brownlow Street
Liverpool, L69 3GP, UK

Clark, Julian D.
Chevron
San Ramon, California, USA

Gardiner, Andrew
Petroleum Engineering Institute
Heriot-Watt University
Edinburgh, EH14 4AS, UK

Abstract

With deep-water basins becoming mature exploration areas, and the number of undrilled structural traps diminishing, stratigraphic traps are growing increasingly important. Onlapping turbidite sands are a common stratigraphic trap type in confined basins; however, onlap architecture can assume a number of different geometrical and facies characteristics as a result of interactions between the turbidity currents and the onlap surface. These variations have important implications for the accumulation and trapping of hydrocarbon reserves, in that the variety affects the quality and recognition of good onlap seal.

To investigate stratigraphic traps in turbidite systems, the spectacularly exposed, seismic-scale Montagne de Chalufy onlap section in the Grès d'Annot turbidite system of the French Alps is used to generate various forward synthetic seismic 2D sections. Three parameters are varied independently: input model detail, seismic impedance contrast, and dominant wavelet frequency. Seismic velocity and rock density values are taken from producing reservoirs to represent the observed lithologies in the Grès d'Annot. The three petroleum reservoir scenarios investigated are a Plio-Pleistocene Gulf of Mexico reservoir and Tertiary and Jurassic North Sea reservoirs. Two levels of 2D input model detail are investigated: 1) a detailed model having observed structural and sedimentary complexities to test vertical and lateral seismic resolution, and 2) a simple onlap model without the complexities. Two Ricker wavelet dominant frequencies are chosen, 26 and 50 Hz. Synthetic seismic results show outcrop analogues of turbidite sandstone reservoirs can be usefully converted to forward seismic sections. 2D seismic sections generated from high frequency wavelets allow subsequent geological interpretations that almost replicate detailed input models, although onlap termination or drape was still difficult to resolve. Gross architectures of massive, onlapping, turbidite sandstones may still be resolved in low frequency seismic datasets.

Introduction

Confined, deep-water basins can be produced by any combination of salt-, mud- and tectonic deformation (*e.g.*, Gulf of Mexico, offshore Niger delta, and offshore Baram delta, Borneo). Stratigraphic traps in these basins are often dependent on relationships between deep-water strata and the slopes that define the basin. Deep-water strata typically onlap the margin of the confined basin, but precise onlap relationships can be difficult to resolve, particularly in salt provinces where salt margins are often steep and are therefore difficult to resolve faithfully in seismic data. Important details of onlap relationships may be obscured in these situations, leading to uncertainty concerning reservoir charge and seal.

In these circumstances exposed examples of onlap surfaces can provide insights into onlap relationships and aid understanding of the seismic expression of the surfaces. Forward seismic models of large-scale, outcrop exposures have been generated by other authors (Batzle and Gardner, 2000; Coleman *et al.,* 2000; Bourgeois *et al.,* 2004; Schwab *et al.,* 2007) to allow both geologists and geophysicists to compare how much high-resolution outcrop data are usually imaged in seismic data of comparable reservoir intervals. However, to date, an exposed onlap surface has not been modeled. The Montagne de Chalufy turbidite onlap in the Haute Provence Region of the French Alps is a spectacular, seismic-scale exposed onlap surface that can be use-

fully converted to a synthetic seismic section. The exposure has been field investigated, interpreted, digitized, and modeled, to generate forward seismic 2D sections.

Geological setting

The Grès d'Annot turbidite system is preserved in a series of north-south aligned exposed remnants (Fig. 1), a result of the Tertiary Alpine thrust-sheet-top basin province that developed by response to loading in front of the southwest-directed Alpine fold-belt (Apps, 1987). During the Eocene-Oligocene, the Alpine foreland basin was ~160 km long, ~80 km wide and orientated approximately northwest-southeast. The early Eocene basin fill sequence consists of a deepening succession of carbonates; firstly the shallow water Calcaires Nummulitiques Formation followed by deeper water paleoslope and basinal marls known as the Marnes Bleues Formation. Later Marnes Brunes Inférieures Member and succeeding Grès d'Annot Formation represent the onset and main phase of clastic input that was primarily fed with sediments from the south (Stanley, 1975; Elliott *et al*., 1985; Ravenne *et al*., 1987).

The Marnes Brunes Inférieures (or Lower Brown "Marls") represented a mixture of continued pelagic Marnes Bleues deposition and early phase turbidite clastics and are thus typically composed of 40% clastic sands (Stanbrook and Clark, 2004). At Montagne de Chalufy, the Marnes Brunes Inférieures is succeeded by, and intercalated with the Grès d'Annot Formation, which consists of coarse-grained, sand-rich turbidity current deposits and associated sediments. The Grès d'Annot Formation is predominantly sand-rich and typically coarse-grained.

The Montagne de Chalufy onlap section is at the southernmost end of the Trois Evêchés subbasin, one of a series of outliers in the Grès d'Annot turbidite system in southeast France (Fig. 1). The Trois Evêchés outlier is generally considered to be a subbasin (Apps *et al.*, 2004), positioned at the distal end of the exposed Grès d'Annot turbidite system, with sediments being fed from the Grand Coyer subbasin to the north (Fig. 1).

Relatively steep and structurally complex Marnes Bleues Formation palaeoslopes (typically 8º–15º dips; Hilton and Pickering, 1995) have been found within the Grès d'Annot system, possibly by virtue of a high-carbonate content, estimated at 65% (Ravenne *et al.,* 1987), which would have led to partial and early lithification of the Marnes Bleues sediments.

The Montagne de Chalufy onlap

At the southernmost end of Trois Evêchés is Montagne de Chalufy onlap section. This section is a well-known and documented onlap (Elliott *et al.,* 1985; Apps, 1987; Sinclair 1994; Hilton and Pickering, 1995; Pickering and Hilton, 1998; Joseph and Ravenne, 2001; Smith and Joseph, 2004, Puigdefàbregas *et al.,* 2004). Montagne de Chalufy offers a seismic scale section of an onlap surface at the contact of Marnes Bleues with the Marnes Brunes Inférieures/Grès d'Annot. The exposed trend of the onlap surface is from northwest-southeast, and the onlap surface can, with difficulty, be restored to northeast-southwest strike, dipping to the northwest. Paleoflow was to the west-northwest, slightly oblique to the dip of the onlap surface. An 800 m long, 150 m high section of the onlap surface is considered in this work (Fig. 2).

Montagne de Chalufy exposes a locally steep sector of the onlap surface that is highlighted by abrupt terminations of three turbidite sandstone bodies; this sector of the onlap surface lies above a thrust repetition of the Marnes Bleues that produced additional relief on the surface (Apps, 1987). The sandstone bodies, separated by units of brown shale and thin-bedded turbidites (Marnes Brunes Inférieures), apparently onlap towards the south-southeast (Fig. 2). The observed relationship is complicated by a fault that results in a repetition of the onlap of the middle sandstone body. Puigdefàbregas *et al.,* 2004 argue that the fault is normal which is in keeping with other known normal faults in the vicinity.

The lowermost sand body (SB1) is up to 35 m thick and contains, in the lower and upper part, thick-bedded, graded and massive sandstones interpreted as the deposits of high-density turbidity currents. The middle part of SB1 is more shale-rich and consists of thinner bedded, lower density, Bouma-type turbidites (Fig. 3A). This sector of the onlap is relatively steep and sandstone beds in SB1 retain their thickness in close proximity to the slope with beds onlapping the surface abruptly and terminating over a distance of 1–2 m (Fig. 2B).

The second sand body (SB2) is 10–12 m thick and onlaps a more gently dipping sector of the onlap surface. The thickness of the sandstone body is retained across the exposure, but then thins gradually for 120 m before terminating against the onlap surface (Fig. 2B). The final termination is abrupt and again involves the final bed base rising steeply against the onlap surface (Fig. 3B). The lower part of SB2 comprises coarser grained, high density turbidites with inversely graded lower divisions that correspond with the traction carpet layers of Lowe, 1982 (Fig. 3C). The upper part of this body is dominated by a large-scale slump fold (Joseph and Ravenne, 2001; Smith and Joseph, 2004).

In sectors where the onlap surface is a contact between the Marnes Bleues and the Marnes Brunes Inférieures (the later vertically separating the sandstone bodies), the contact is cryptic by comparison. Blue-gray marls containing slightly varying carbonate content

(Marnes Bleues) are abruptly but cryptically overlain by marls with a lower carbonate content and thin, centimeter-scale turbidite sandstone beds that become thicker and more common upwards (Fig. 4).

Methodology

Forward Seismic Modeling (also known as synthetic seismic) in this study involves the collation of outcrop data in the form of large-scale photomontages that are then interpreted to produce a detailed, 2D architectural interpretation of the outcrop exposure. The initial interpretation is then validated by both field ground-truth investigations and detailed sedimentary outcrop logs that also provide high-resolution, 1D data. The detailed architectural interpretation and the chosen dominant seismic wavelet frequency is then fed into specialist software that convolves the model into a seismic section, using user input, seismic impedance contrasts between different lithologies. Seismic impedance contrast can then be calculated using published velocity and density values for the different lithological types in the selected section, enabling the rock values to be varied in order to simulate the petroleum reservoir under consideration. The geoscientist can also vary the frequency to simulate the depth and/or quality of seismic available. Overburden can also be added to simulate real-world situations.

The Montagne de Chalufy outcrop had initially been field investigated and interpreted as a 2D cross section (with adjustment for photomontage perspective). Two sedimentary interpretations were investigated (Pringle, 2003); a complete model retaining observed faults and heterolithic intervals, and a simple model in which the structural complexities and the heterolithic detail removed. The more detailed model had both turbidite thin-bedded intervals within the sand-rich intervals and structural (fault) complications preserved over the four onlapping (including the onlap repetition as a result of the faulting), undeformed, massive sandstone bodies (Fig. 5). The simple model did not attempt to preserve either the heterolithic intervals or the faulting (Fig. 6).

The interpreted models were subsequently digitized and then processed using GMAplus STRUCT[1] software program. A number of parameters were tested; the simplest being the potential vertical seismic resolution differences that would be produced using different dominant frequencies. The modeling program expected average velocity and density values for each bedding unit. Three reservoir unit types were modeled; massive sandstones, massive shale intervals and interbedded turbidite sandstones and shales. It was decided to use velocity values from three producing reservoirs, as the aim was to simulate conventional seismic information through reservoirs with comparable seismic impedance values.

1. Now GeographiX™

The three producing reservoirs were the Forties Field, a Tertiary North Sea (UKCS) reservoir; the Magnus Field, a Jurassic, North Sea (UKCS) reservoir; and the Mars Field, a Plio-Pleistocene, Gulf of Mexico reservoir. Values for the three reservoirs were obtained from published data from Jager *et al.,* (1997), Partington *et al.* (1993), and Chapin (1996), respectively. These values (as well as comparable data obtained from other authors) are detailed in Figure 7. The underlying Cretaceous basement values used were constant for all models (Fig. 7), and checked against Badley (1948) values for similar lithologies. Although the underlying Marnes Bleues Formation was observed to be dominantly composed of marls, these units were modeled as "fast shales" as may be seen in the geological record in areas with long periods of nonclastic deposition.

Two dominant Ricker wavelet frequencies were chosen for this study, a 26 Hz and 52 Hz wavelets, to represent higher and lower frequency seismic datasets. Synthetic traces were spaced at 12.5 m—equivalent to an inline surface seismic section. Vertical incidence, zero-offset rays were used to give the appearance of a seismic profile without the complexities of dip moveout and migration, which commonly occur in standard, seismic Common Mid-Point (CMP) data.

Results

Figure 8 shows two synthetic seismic sections, generated using 26 and 52 Hz Hz dominant frequency wavelet based on the original interpretation using lithological parameters of a Plio-Pleistocene Gulf of Mexico analogue (the Mars Field). Figure 9 shows two synthetic seismic sections, generated using 26 and 52 Hz Hz dominant frequency wavelet based on the original interpretation using lithological parameters of a Jurassic North Sea analog (the Magnus Field). Figure 10 shows two synthetic seismic sections, generated using 26 and 52 Hz Hz dominant frequency wavelet based on the original interpretation using lithological parameters of a Tertiary North Sea analogue (the Forties Field). Figure 11 shows two synthetic seismic sections, generated using 26 and 52 Hz Hz dominant frequency wavelet based on the original interpretation with faults removed using the same Tertiary North Sea analog (Forties Field).

The brightest amplitudes (and hence largest impedance contrasts) were found in models representing the Jurassic North Sea reservoirs. However, overall variations in impedance values seem to have little effect on results at the high Signal/Noise Ratios (SNR) used.[1] The massive sandstone bodies of the Grès d'Annot could be identified on all sections, at both high and low frequencies. At the higher frequency (50 Hz), the variations in sandstone body thickness could also be resolved. The small thrust offset (in the original

1. Noise was not added to any of the models.

detailed model) could be distinguished in all high frequency synthetic sections. Note that such a high frequency (50 Hz) signal would not normally be returned from deep Jurassic targets in the North Sea. The Jurassic North Sea reservoir parameters show high velocity values, and hence a tighter synthetic seismic section. Comparison of time values for the Cretaceous basement in Figure 8 with Figure 9 shows a TWT of 0.28 and 0.25 respectively.

Discussion

From analysis of the synthetic seismic section results, resolving onlapping sandstone units on seismic sections is a potential problem. Using typical seismic frequencies of 26 Hz, only the large-scale, sand-rich intervals could be successfully differentiated from the background materials. The onlap relationship of these bodies onto paleoslopes and other potentially topographically complex basin floors could not be recognized or resolved, which is crucial when defining stratigraphic traps. The internal, sand-poor heterolithic intervals were also not well resolved, which may cause petroleum geologists to overestimate potential reserves.

The higher 52 Hz frequency data produced much improved vertical and horizontal seismic resolution, as both the heterolithics intervals and the major fault were imaged, although the small faults were not resolvable. The Gulf of Mexico and Tertiary North Sea analogs (Figures 8 and 10, respectively) were generally similar, both being at a relatively shallow stratigraphic depth, whereas the Jurassic North Sea analogs (Figure 9) showed the poorest resolution as would be expected from a deeper reservoir.

Sedimentological and structural data, observed in the field by geoscientists working on outcrop analogs, often give far higher resolution than is observed in conventional seismic data, and what looks like relatively simple sedimentology and structural data to the geophysicist can, in fact, be much more complicated and unimaged. An improvement to this modeling exercise would be to add seismic “noise” to make the 2D sections more realistic and to utilize the collected 1D sedimentary logs to create more realistic seismic wavelets between the different modeled sedimentary intervals.

Conclusion

The overall appearance of the Chalufy onlap surface is imaged effectively in the synthetic seismic data in that the presence of the sandstone bodies, their onlapping nature and the major fault locally offsetting the onlap sandstone bodies are visible in each case. The thickness contrast between SB1 and SB2 is successfully

imaged in all cases, and the abrupt termination of SB1 contrasting with the more gradual thinning of SB2 is also apparent in most cases.

Results show outcrop analogues of turbidite sandstone reservoirs may be effectively converted to forward seismic 2D sections. Seismic model sections generated from high frequency wavelets allow interpretations that almost replicate detailed input geological models. Gross architectures of massive, onlapping, turbidite sandstones may still be resolved in low frequency seismic datasets.

Heterogeneities within onlapping sandstone bodies can result either from external controls, or can be forced locally by interaction with the onlap surface. Important controls on the latter include (Fig. 12): 1) the angle of the onlap surface (Smith and Joseph, 2004); the orientation of the onlap surface in relation to the paleocurrent direction (Kneller and McCaffrey, 1999; Amy *et al.*, 2004), 2) the thickness of flows in relation to the height of the onlap surface (McCaffrey and Kneller, 2001), and 3) the potential for locally triggered slope failures that may initiate slides, slumps and debris flow processes that run out for short distances down the onlap surface and complicate stratigraphic relationships on the surface (Talling *et al.*, 2004; Puigdefabregas *et al.*, 2004).

In the Chalufy example internal heterogeneities of the sandstones bodies are below resolution in the model runs, but the level of heterogeneity forced by interaction with the onlap surface in the Chalufy example is limited (Sinclair, 1994). Flow directions are slightly oblique to the depositional strike of the onlap surface and flow heights are probably low in comparison to the height of the onlap surface. The synsedimentary deformation in SB2 is of localised extent and involves mainly vertical foundering rather than significant lateral translation. The main heterogeneity is a thinner bedded, low net/gross interval in the middle of SB1 that was more distantly or externally forced. In other cases where flows approach onlap surfaces more frontally and are partially ponded, rebound. or reflect, the level of interaction between the flow and the onlap surface will be more substantial and may require image log or core data in order to be recognised and assessed in relation to hydrocarbon migration, sealing and reservoir impact.

Acknowledgments

Peter Olden gave guidance on the use of GMA. Robin Westerman and Leon Barens related the convolutional model used by GMA to the wider context of wave-field modeling and of surface seismic acquisition and processing practice. The Heriot-Watt University Genetic Units Project (GUP) and GEOTipe Project, both funded by petroleum-industry consortia, are acknowledged for financial support for J. Pringle for this study. Nautilus UK Ltd is acknowledged for the use of drafted materials.

References

Amy, L.A., W.D. McCaffrey, and B.C. Kneller, 2004, The influence of a lateral basin slope on the depositional patterns of natural and experimental turbidity currents, *in* P. Joseph and S.A. Lomas, eds., Deep-water sedimentation in the Alpine Foreland Basin of SE France: new perspectives on the Grès d'Annot and related systems: Geological Society London Special Publication 221, p. 311-330.

Apps, G., 1987, Evolution of the Grès d'Annot basin, SW Alps: University of Liverpool PhD dissertation, 451 p.

Apps, G., F. Peel, T. Elliott, 2004, The structural setting and palaeogeographic evolution of the Grès d'Annot basin, *in* P. Joseph and S. Lomas, ed., Deep-Water Sedimentation in the Alpine Foreland Basin of SE France: New Perspectives on the Grès d'Annot and Related System:.Geological Society of London Special Publication 221, p. 65-96.

Badley, M.E., 1948, Practical seismic interpretation, Boston, USA, 266 p.

Batzle, M. and M.H. Gardner, 2000, Lithology and fluids: seismic models of the Brushy Canyon Formation, West Texas, *in* A.H. Bouma and C.G. Stone, ed., Fine-Grained Turbidite Systems: AAPG Memoir 72, p. 127–142.

Bourgeois, A., P. Joseph, and J-C. Lecomte, 2004, Three-dimensional full wave seismic modelling versus one-dimensional convolution: the seismic appearance of the Grès d'Annot turbidite system, *in* P. Joseph, and S. Lomas, ed., Deep-Water Sedimentation in the Alpine Foreland Basin of SE France: New Perspectives on the Grès d'Annot and Related Systems: Geological Society Special Publication.

Chapin, M.A., G.M. Tiller, and M.J. Mahaffie, 1996, 3-D architecture modeling using high-resolution seismic data and sparse well control: examples from the Mars "Pink" Reservoir, Mississippi Canyon area, Gulf of Mexico, *in* P. Joseph, and S. Lomas, ed., Applications of 3-D seismic data to exploration and production: AAPG Studies in Geology No. 42, AAPG/SEG Joint Publication, Tulsa, Oklahoma, 5, p. 123-131.

Coleman, J.L., F.C. Sheppard III, and T.K. Jones, 2000, Seismic resolution of submarine channel architecture as indicated by outcrop analogues *in* A.H. Bouma and C.G. Stone, ed., Fine-Grained Turbidite Systems: AAPG Memoirs 72, p. 119–126.

Elliott, T., G. Apps, H. Davies, M. Evans, G. Ghibaudo, and R.H. Graham, 1985, A structural and sedimentological traverse through the Tertiary foreland basin of the external Alps of southeast France, *in* P.A. Allen and P. Homewood, ed., Field excursions Guidebook for the International Association of Sedimentologists meeting on foreland basins, Fribourg p. 39-73.

Hilton, V. C., and K.T. Pickering, 1995, The Montagne de Chalufy turbidite onlap, Eocene-Oligocene turbidite sheet system, Hautes Provençe, SE France, *in* K.T. Pickering, R.N. Hiscott, N. Hl.Kenyon, and R.D.A. Smith, ed., Atlas of Deep Water Environments: Architectural style in turbidite systems: Chapman & Hall, London, p. 236-241.

Jager D.H., *et al.*, 1997, Variety of turbidite deposits within the Forties Fan: examples from the Nelson Field, *in*

C.D. Oakman, J.H. Martin, and P.W.M. Corbett, ed., Cores from the NW European Hydrocarbon Province: an illustration of geological applications from exploration to development: Geological Society of London, p. 175-180.

Joseph, P., and S.A. Lomas, 2004, Deep-water sedimentation in the Alpine Foreland Basin of SE France: new perspectives on the Grès d'Annot and related systems: an introduction, *in* P. Joseph and S.A. Lomas, eds., Deep-water sedimentation in the Alpine Foreland Basin of SE France: new perspectives on the Grès d'Annot and related systems: Geological Society London Special Publication 221, p. 1-16.

Joseph, P., and C. Ravenne, 2001, (Excursion D) Chalufy, *in* P. Joseph and S. Lomas, ed., Turbidite sedimentation in confined settings, Research meeting & field excursion to the Grès d'Annot, Nice, France, September

Kneller, B.C., and W. McCaffery, 1999, Depositional effects of flow nonuniformity and stratification within turbidity currents approaching a bounding slope: Deflection, reflection, and facies variation: Journal Sedimentary Research, v. 69, no. 5, p. 980-991.

Partington M.A., P. Copestake, B.C. Mitchener and J.R. Underhill, 1993, Genetic sequence stratigraphy for the North Sea Late Jurassic and Early Cretaceous: distribution and prediction of Kimmeridgian-Late Ryazanian reservoirs in the North Sea and adjacent areas, *in* J.R. Parker ed., Petroleum Geology of Northwest Europe: Proceedings of the 4th Conference, The Geological Society, London, 1, p. 347-370.

Pickering, K. T. and V.C. Hilton, 1998, Turbidite Systems of Southeast France: Vallis Press, London, 229 p.

Pringle, J. K., 2003, Integrated techniques for the acquisition and visulaisation of 3D meso- to macro-scale sedimentary architectures of petroleum reservoir outcrop analogues: Institute of Petroleum Engineering, Heriot-Watt University Unpublished PhD dissertation, 326 p.

Puigdefàbregas, C., J. Gjelberg, and M. Vaksdal, 2004, The Grès d'Annot in the Annot syncline: outer basin-margin onlap and associated soft-sediment deformation, *in* P. Joseph, and S. Lomas, ed., Deep-Water Sedimentation in the Alpine Foreland Basin of SE France: New Perspectives on the Grès d'Annot and Related Systems: Geological Society Special Publication 221, p. 367-388.

Ravenne, C., R. Vially, P. Riché, and P. Trémolières, 1987, Sédimentation et tectonique dans le basin marin Eocène Supérieur-Oligocène des Alpes du sud : Revue de l'Institut Français du Pétrole, 42, p. 529-553.

Ravenne, C., P. Joseph, and O.G. de Souza, 1995, Classic Annot sandstones: Seismic scale exposures of the Eocene basinal turbidites in the French external Alps: American Association of Petroleum Geologists International conference and exhibition, Nice, IFP.

Schwab, A.M., B.T. Cronin, and H. Ferreira, 2007, Seismic expression of channel outcrops: offset stacked versus amalgamated channel systems: Marine and Petroleum Geology, 24, p. 504-514.

Sinclair, H. D., 1994, The influence of lateral basinal slopes on turbidite sedimentation in the Annot Sandstones of SE France: Journal of Sedimentary Research, A64 (1), p. 42-54.

Smith, R., and P. Joseph, 2004, Onlap stratal architectures in the Grès d'Annot: Geometric models and controlling factors, *in* P. Joseph, and S. Lomas, ed., Deep-Water

Sedimentation in the Alpine Foreland Basin of SE France: New Perspectives on the Grès d'Annot and Related Systems: Geological Society Special Publication 221.

Stanley, D. J., 1975, Submarine canyon and slope sedimentation (Grès d'Annot) in the French Maritime Alps: 9th International Sediment Congress, Nice, France, p. 131.

Stanbrook, D.A., 2003, The geology of Grand Coyer, Southeast France. Relationships between basin floor topography and the deposition of the Grès d'Annot and Marnes Brunes Inférieures: Heriot-Watt University Unpublished PhD dissertation, 302 p.

Stanbrook, D. A., and J.D. Clark, 2004, The Marnes Brunes Inférieures in the Grand Coyer remnant: characteristics, structure and relationship to the Grès d'Annot, *in* P. Joseph, and S. Lomas, ed., Deep-Water Sedimentation in the Alpine Foreland Basin of SE France: New Perspectives on the Grès d'Annot and Related Systems: Geological Society Special Publication.

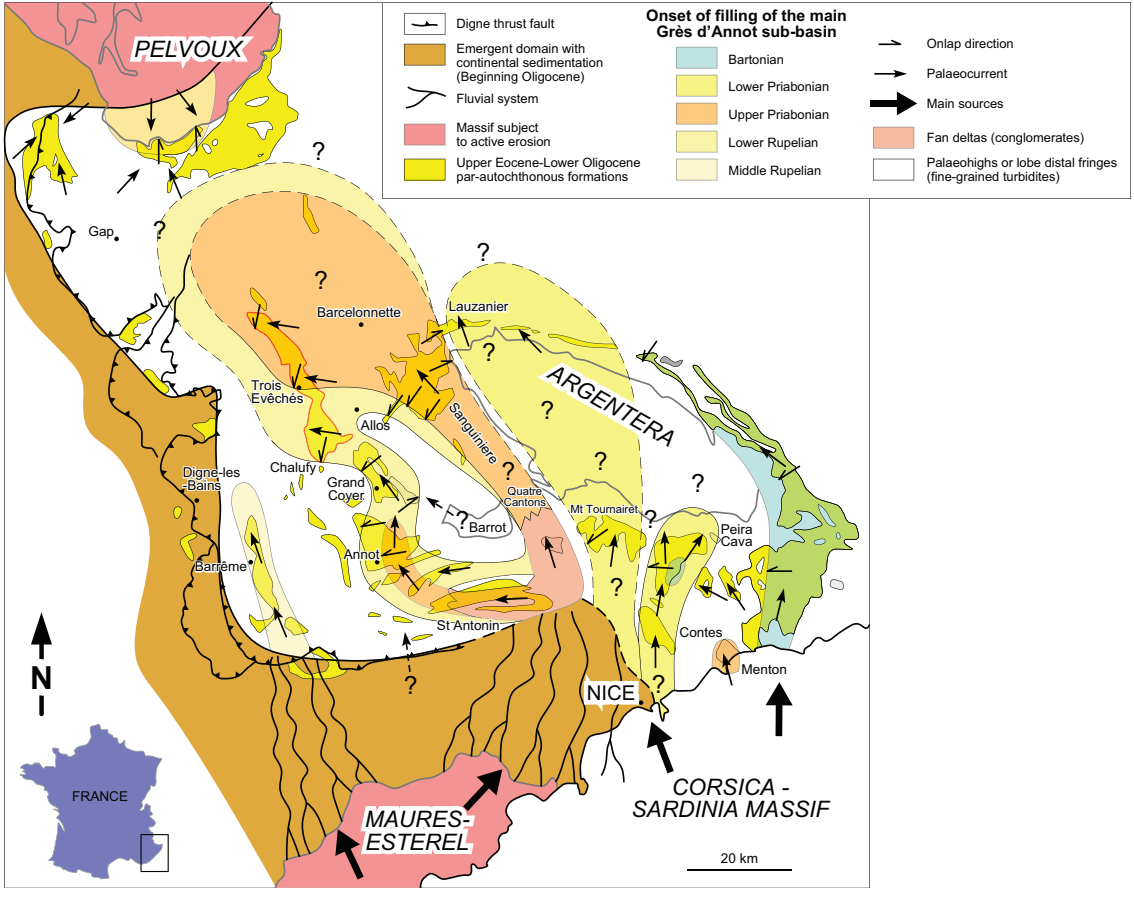

Figure 1. Map of evolving sediment transport paths of the Grès d'Annot basin; note the position of Chalufy at the southern end of the Trois Evêchés sub-basin that represents the distal part of the St Antonin sediment pathway. Modified from Joseph and Lomas, 2004.

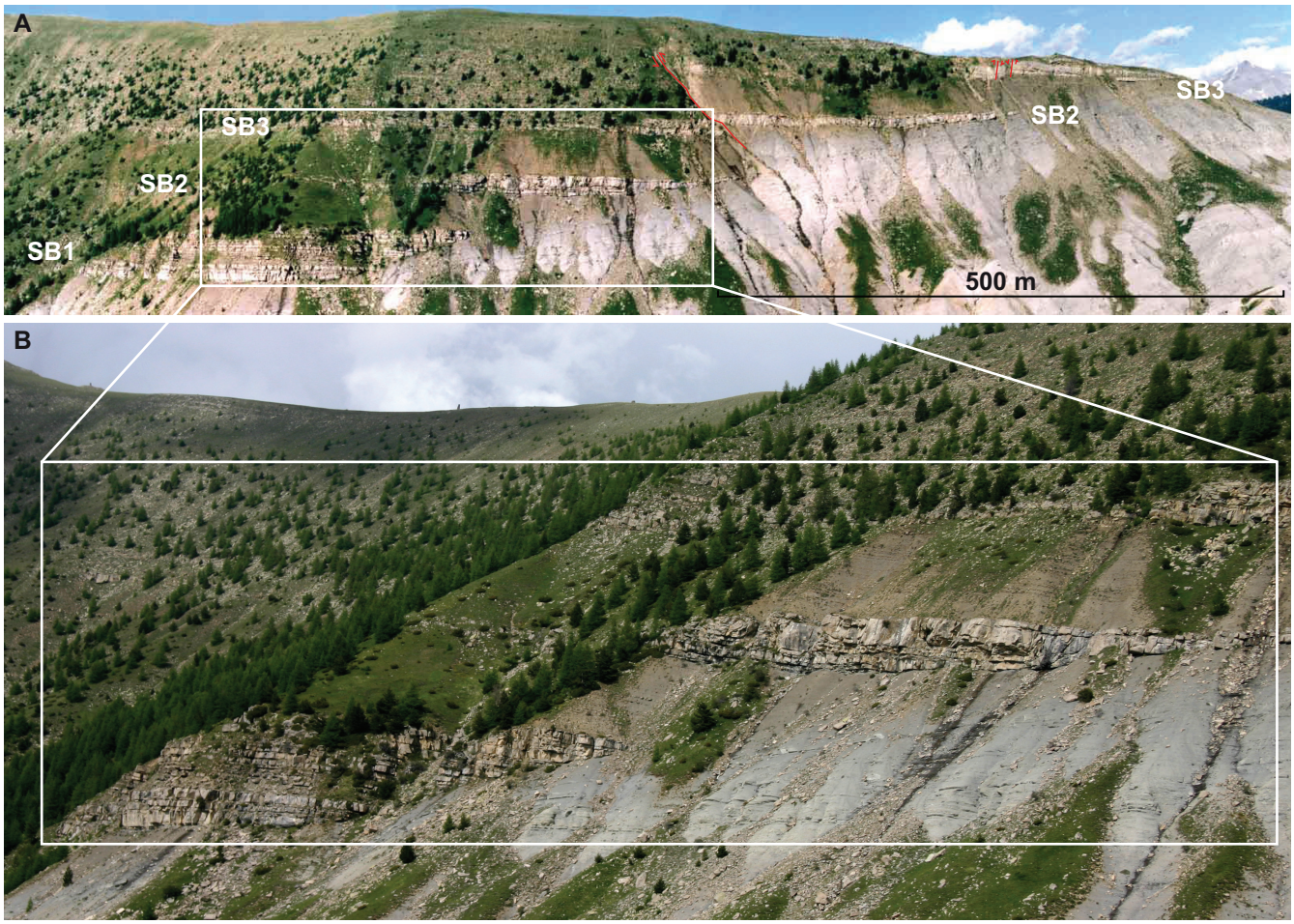

Figure 2. The Montagne de Chalufy onlap section; the foreland basin into which the Grès d'Annot was deposited had a complex basin-floor topography, which controlled the distribution of sand bodies. Onlaps similar to that at Chalufy are common throughout the area. (A) Note the onlap of sandstone packets within the Grès d'Annot onto the Marnes Bleues slope. The slope was produced by Tertiary deformation, and controlled by thrust propagation in the underlying Cretaceous succession. Geometry is complicated by oblique-slip faults, causing repetition of the middle sand body onlap on both sides of the main fault (annotated). (B) View of Sandstone Bodies 1 and 2 onlapping a surface on the top Marnes Bleues. Note the abrupt termination of Sandstone Body 1, the more gradual thinning of Sandstone Body 2, and the cryptic marl-on-marl contact (Marnes Bleues/Marnes Brunes Inférieures) in sectors between the sandstone bodies.

Figure 3. (A) Typical appearance in the field of Sand body 1, showing T_b, commonly erosive-based, coarse-grained sandstone interval fining-up into T_{c-e} medium-grained, wavy and cross-laminated sandstones, inter-bedded with silt and shales. Note plentiful, but commonly isolated, mud-clast present throughout the sandstones. 20 cm card for scale. (B) Final, abrupt termination of Sandstone Body 2 against the onlap surface. Note the abrupt rise of the basal erosion surface (see Figure 2B for context of the termination). (C) Inverse grading produced in a traction carpet layer at the base of a high density turbidite sandstone bed in the lower part of Sandstone Body 2.

Figure 4. Marl-on-marl cryptic contact (Marnes Bleues/Marnes Brunes Inférieures) on the onlap surface above Sandstone Body 2 (mid-left). Bedding in the Marnes Bleues is related to variations on carbonate content of the marls; bedding in the Marnes Brunes Inférieures is related to thin turbidite sandstone beds that become thicker and more common upwards (see section directly above Sandstone Body 2). The precise level of the contact is highlighted by the person pointing.

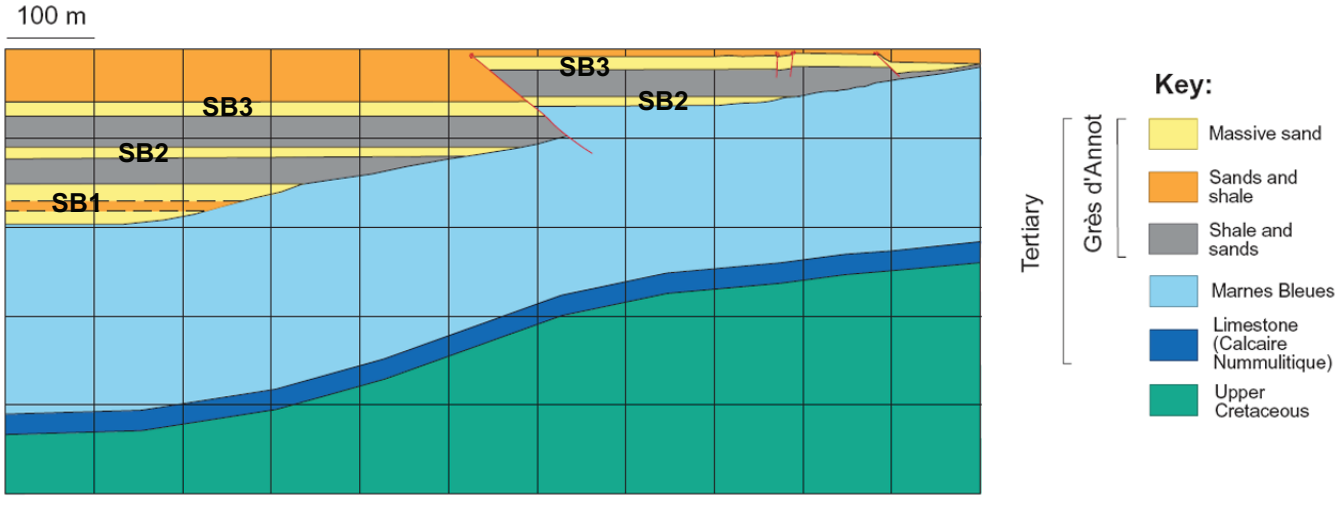

Figure 5. Detailed 2D input model showing both structural interpretation and thin-bedded heterolithics present within the sand-rich intervals (representing the Marnes Brunes Inférieures and Grès d'Annot facies respectively). Note the scale is the same for xy.

Basement Parameters used for all models

	Velocity (m/s)	Density (g/cc)	Impedance (kg m^{-2} s^{-1})
Calcaire Nummulitique	5500	2.66	14630 x 10^3
Upper Cretaceous	5000	2.60	13000 x 10^3

Jurassic North Sea Parameters

	Velocity (m/s)	Density (g/cc)	Impedance (kg m^{-2} s^{-1})
Massive Sand	4233	2.43	10286 x 10^3
Shale and Marl	3110	2.53	7868 x 10^3
Interbedded sands & shales	3858	2.48	9568 x 10^3

Gulf of Mexico Parameters

	Velocity (m/s)	Density (g/cc)	Impedance (kg m^{-2} s^{-1})
Massive Sand	3672	2.08	7628 x 10^3
Shale and Marl	2650	2.25	5692 x 10^3
Interbedded sands & shales	3387	2.13	7214 x 10^3

Tertiary North Sea Parameters

	Velocity (m/s)	Density (g/cc)	Impedance (kg m^{-2} s^{-1})
Massive Sand	3208	2.17	6961 x 10^3
Shale and Marl	2498	2.35	5870 x 10^3
Interbedded sands & shales	2903	2.27	6590 x 10^3

Figure 6. Seismic parameters from producing fields used in this study to represent the different formations associated with the onlap.

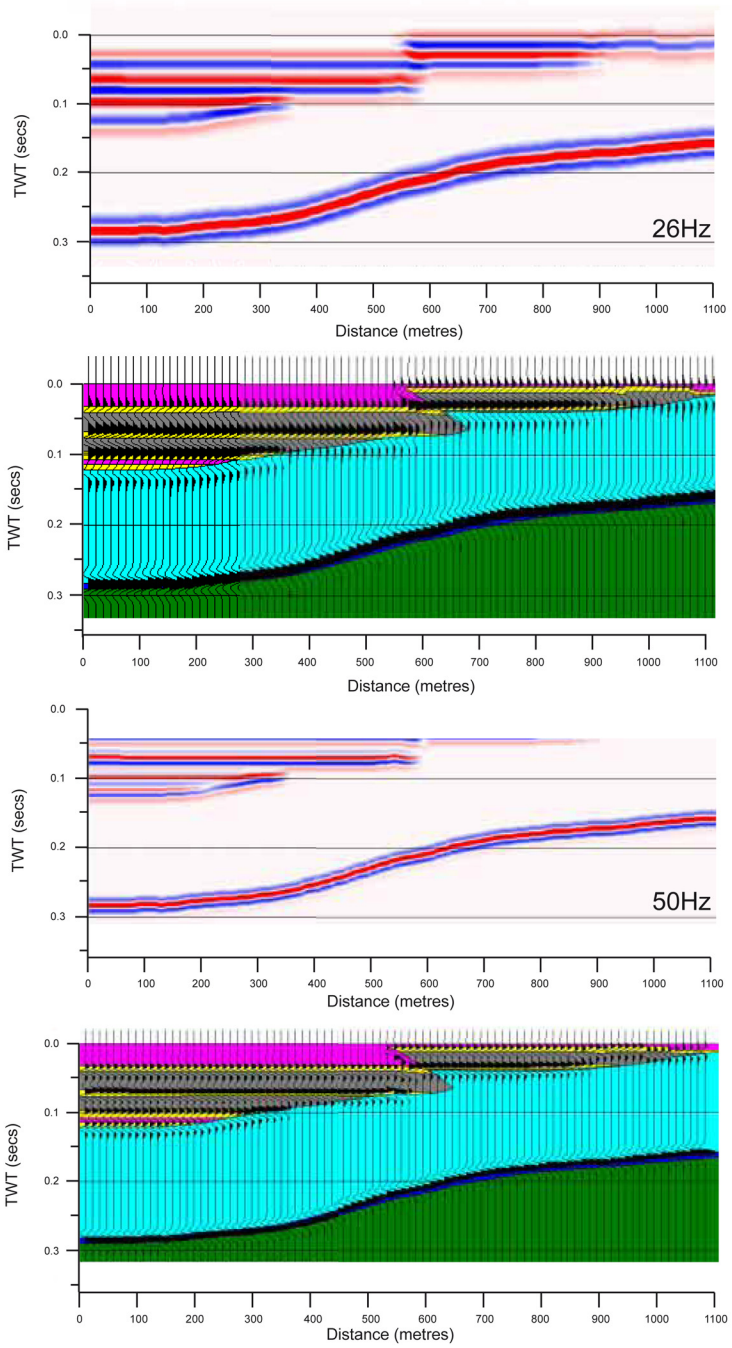

Figure 7. Detailed model Plio-Pleistocene Gulf of Mexico analogue output from GMAplus STRUCT™ software showing (A/B) 26 Hz and (C/D) 52 Hz frequencies, showing color impedance and wiggle trace wavelets respectively (see text for description and discussion). Note wavelet sections have interpreted model shown behind as solid colors.

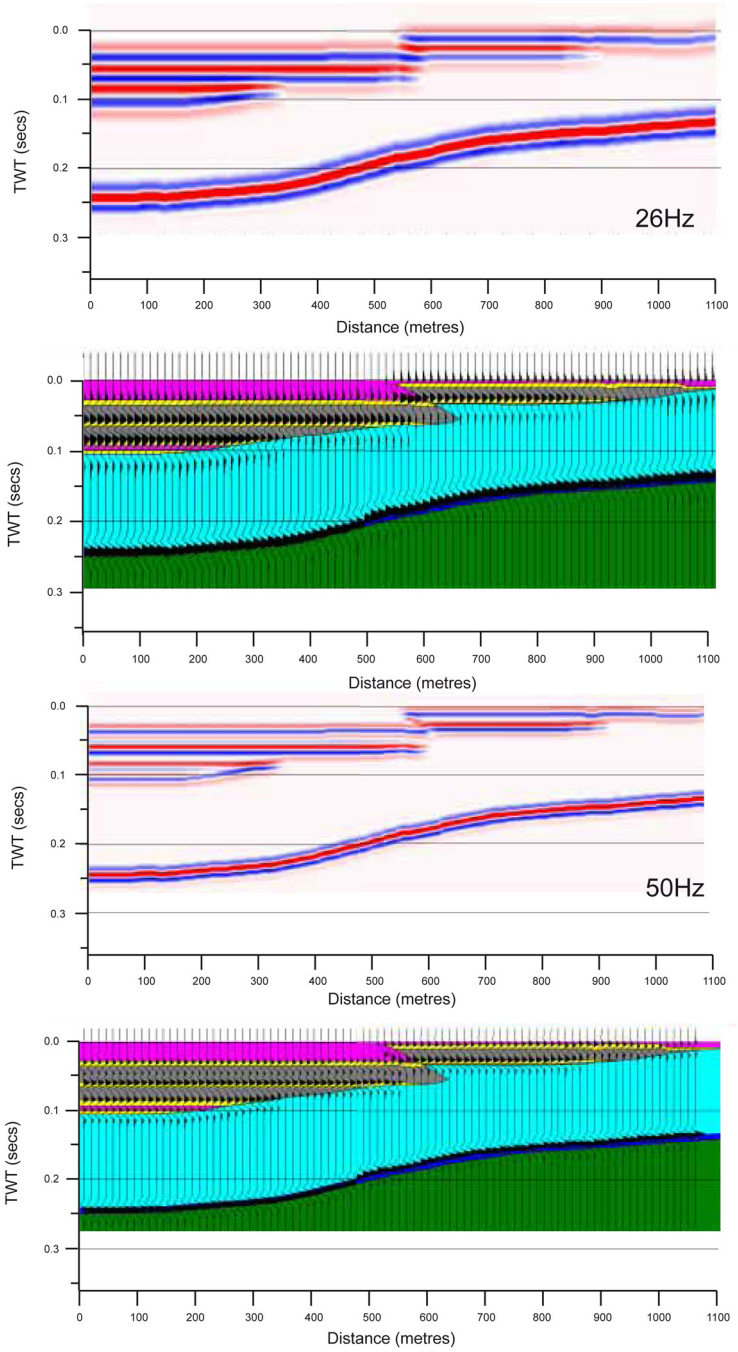

Figure 8. Detailed model Jurassic North Sea analogue output from GMAplus STRUCT™ software showing (A/B) 26 Hz and (C/D) 52 Hz frequencies, showing color impedance and wiggle trace wavelets respectively (see text for description and discussion). Note wavelet sections have interpreted model shown behind as solid colors.

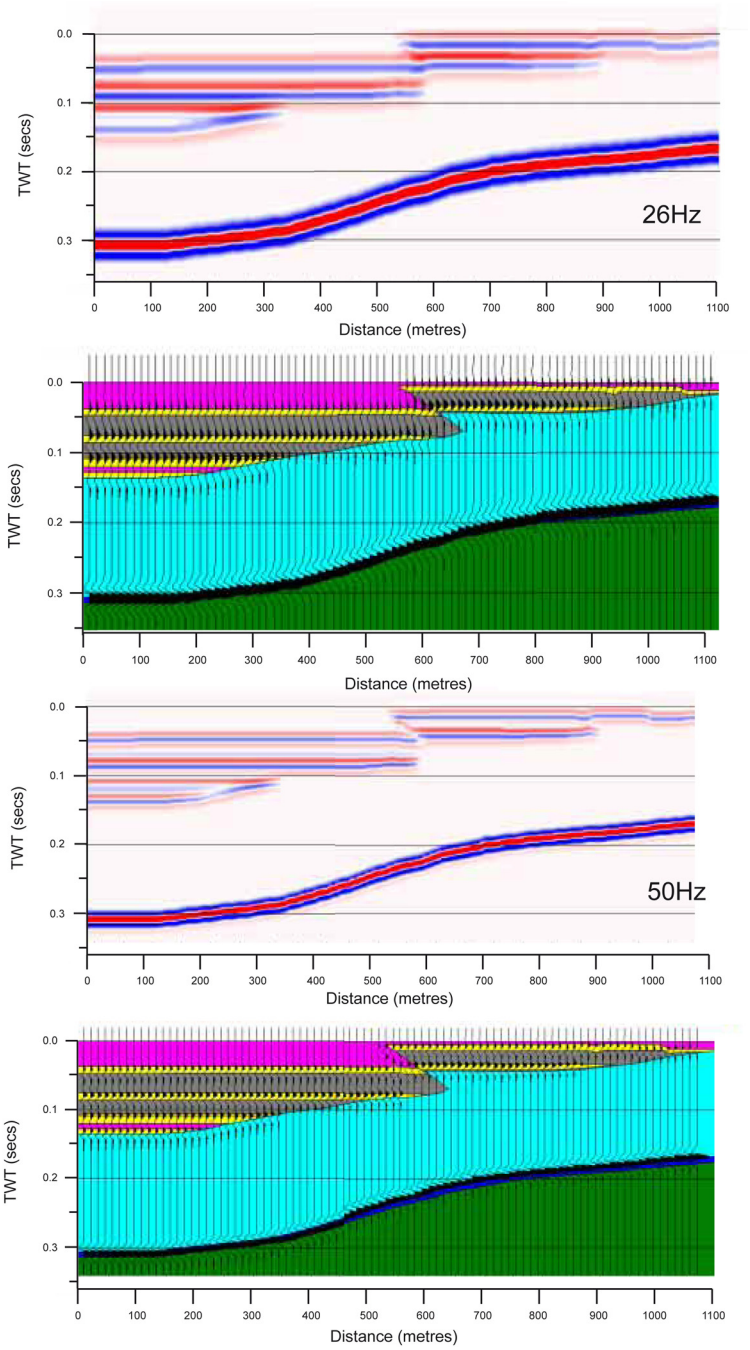

Figure 9. Detailed model Tertiary North Sea analogue output from GMAplus STRUCT™ showing (A/B) 26 Hz and (C/D) 52 Hz frequencies, showing color impedance and wiggle trace wavelets respectively (see text for description and discussion). Note wavelet sections have interpreted model shown behind as solid colors.

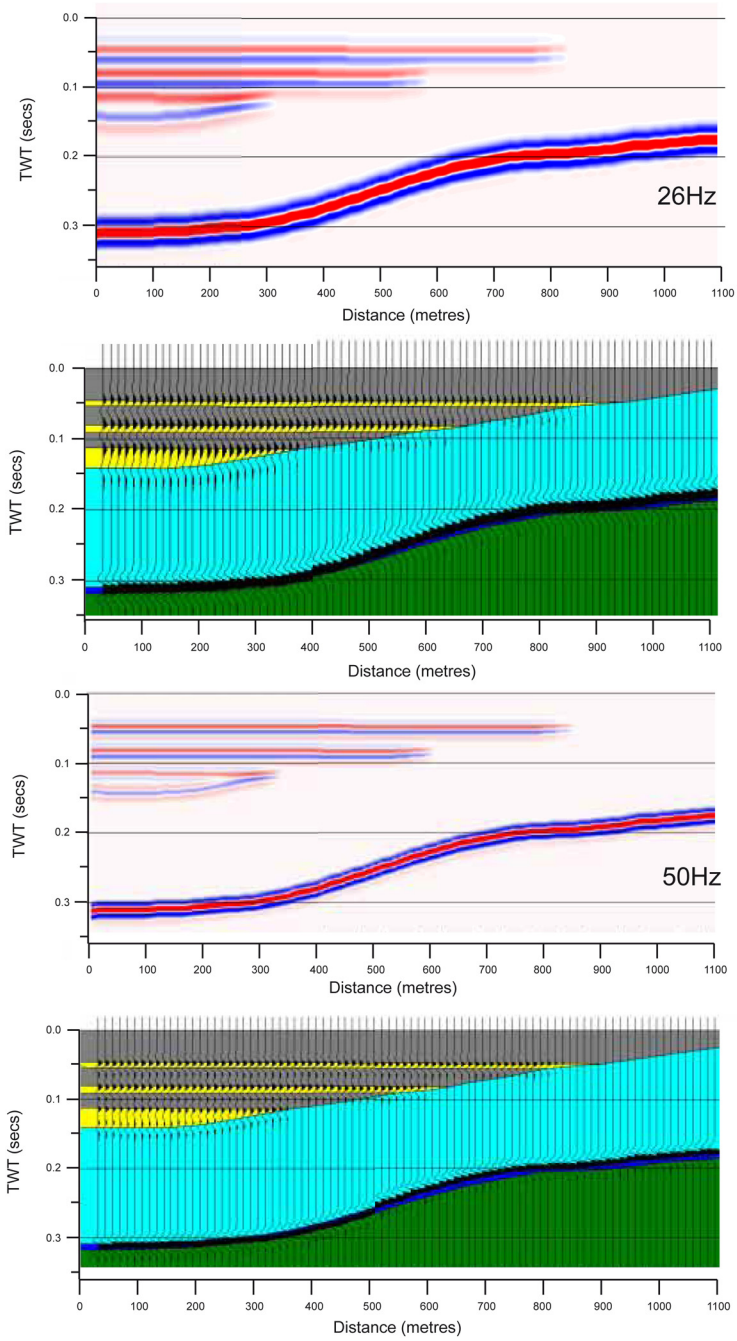

Figure 10. Simplified model (fault detail and heterolithics in lowermost sand removed, compare with Fig. 9) of Tertiary North Sea analogue output from GMAplus STRUCT™ showing (A/B) 26 Hz and (C/D) 52 Hz frequencies, showing color impedance and wiggle trace wavelets respectively (see text for description and discussion). Note wavelet sections have interpreted model shown behind as solid colors.

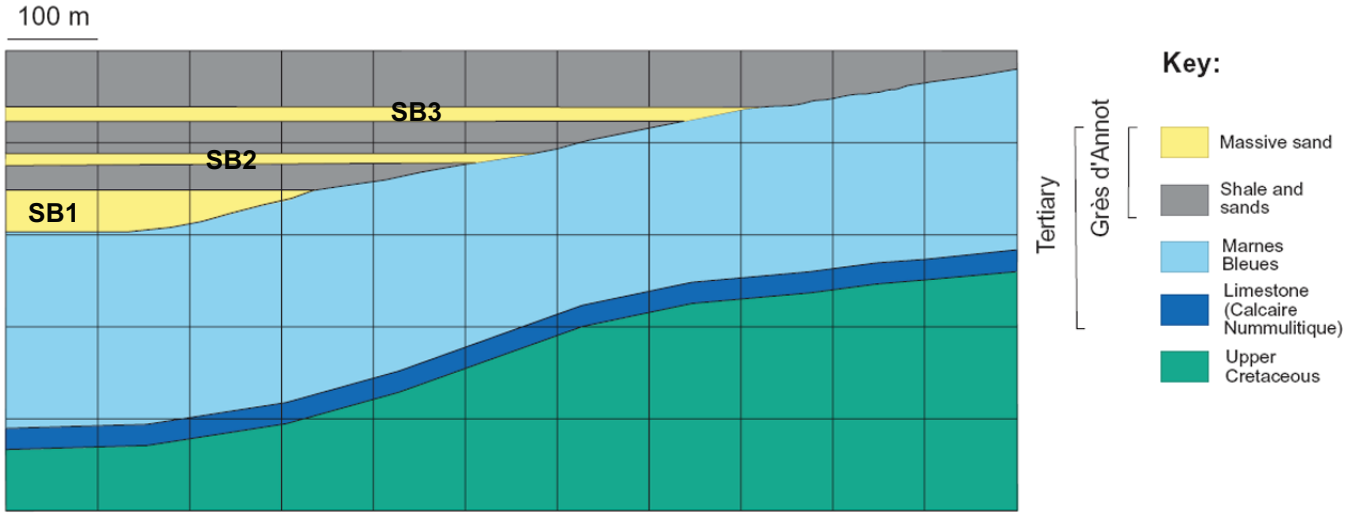

Figure 11. Simple 2D input model, with both structural and detailed heterolithics removed. Note the scale is the same for xy.

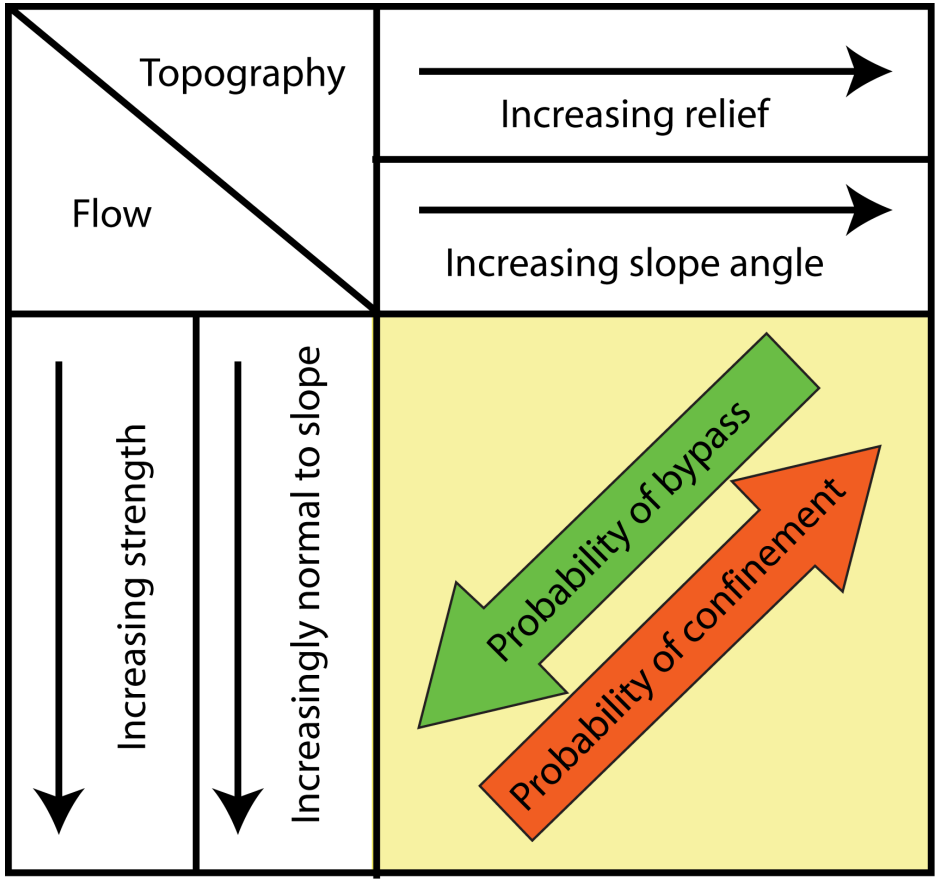

Figure 12. Probability matrix showing the relative likelihood of bypass or confinement of turbidity currents taking into account the parameters of topography (relief, slope angle) and flow (strength and incidence). Modified from Stanbrook (2003).